Functionalized *o*-Quinones: Concepts, Achievements and Prospects

Konstantin Martyanov * and Viacheslav Kuropatov *

G.A. Razuvaev Institute of Organometallic Chemistry of Russian Academy of Sciences, Box-445,
Tropinina str. 49, 603950 Nizhny Novgorod, Russia
* Correspondence: konmart@iomc.ras.ru (K.M.); viach@iomc.ras.ru (V.K.); Tel.: +7-831-462-7682 (V.K.)

Abstract: *o*-Quinones are both well-studied and promising redox-active chelating ligands. There are plenty of interesting effects to be found on *o*-quinone-derived metallocomplexes, such as photo-thermo mechanical effect in solid phase and in solution, luminescence, SMM properties and so on. A combination *o*-quinone function with an additional coordination site or redox active fragment in the same molecule might sufficiently extend an assembling as well as functional capability of such ligand in complexes. In this paper, the authors focus on *o*-quinones decorated with additional non-dioxolene chelating coordination site or with electron donor redox active annelated fragments.

Keywords: *o*-quinone; bifunctional ligands; redox amphoteric ligands; molecular devices

1. Introduction

o-Quinones and their redox forms catecholates and semiquinonates have been continuously studied for many decades (Scheme 1). A rich synthetic chemistry of *o*-quinones provides a nice opportunity for preparation of *o*-quinone-based biologically active compounds for pharmaceutical applications as well as for the construction of novel redox-active ligands for coordination chemistry.
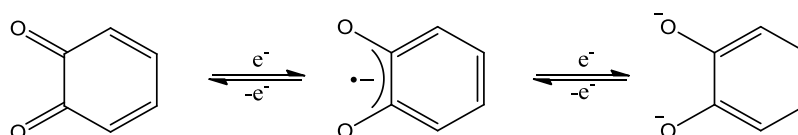
Scheme 1. Redox transformations of *o*-quinone.

The redox nature of *o*-quinone species is a key property that determines their activity in biological systems. *o*-Quinones are involved in oxygen transfer chains in live organisms. In coordination chemistry a redox activity of *o*-quinone ligands is led to relevant applications in material sciences and catalysis. Redox isomerism of metallocomplexes in solid state and solution as well as reversible bending of crystals of Rh and Co semiquinonate complexes are also the result of redox transformations within *o*-quinone ligand [1–3].

From a coordination chemistry point of view *o*-quinones have some useful features: they form stable complexes with almost all metals; moreover they can change formal oxidation state, directly being coordinated to the metal ion. Manipulation of the oxidation state of the *o*-quinone ligand can be realized in different ways, e.g., by optical or thermo-activation, by addition/ displacement/removal of auxiliary ligand in the coordination sphere of the metal ion and so on. A concept of an electron reservoir is typically attributed to *o*-quinone ligands: ligand-centered redox processes provide catalytic activity for *o*-quinone complexes with non-transition metals [4].

Due to these peculiarities, *o*-quinones are promising building blocks for the construction of molecular devices and functional materials. From this point of view a topology of ligand that provides an opportunity for synthesis of coordination polymers or an ordering of the molecules in the crystal phase may be very useful. *o*-Quinone itself might be a bridging ligand in case of binding of metal ions both by dioxolene site and by π-complexation with diene system [5–10]. The chemistry of *o*-quinones is immensely rich and diverse, so there are many ways to functionalize an *o*-quinone molecule. An extension of coordination and functional capabilities of an *o*-quinone molecule by means of introduction of an additional chelating site (i.e., redox-active) is a very promising way. There are several recent papers that describe the synthesis, coordination modes and important properties of bridging di-*o*-quinones (OO~OO) and their isoelectronic analogues di-*o*-iminoquinones (NO~NO) and di-*o*-diimines (NN~NN) [4,11–13]. In this review, we focus on the chemistry and coordination capabilities of bifunctional *o*-quinones decorated with additional alternative chelating coordination sites (NN~OO, SS~OO systems) as well as on annulated di-*o*-quinone assemblies containing an additional redox-active unit.

2. OO~NN Systems

2.1. Coordination Properties of 1,10-Phenanthroline-5,6-dione

One of the first reported examples of such bifunctional ligands is 1,10-phenanthroline-5,6-dione (pdon). This compound was synthesized in 1947 as a byproduct of nitration of 1,10-phenanthroline [14]. Now there is a simple, effective procedure for the preparation of 1,10-phenanthroline-5,6-dione (Scheme 2) [15].
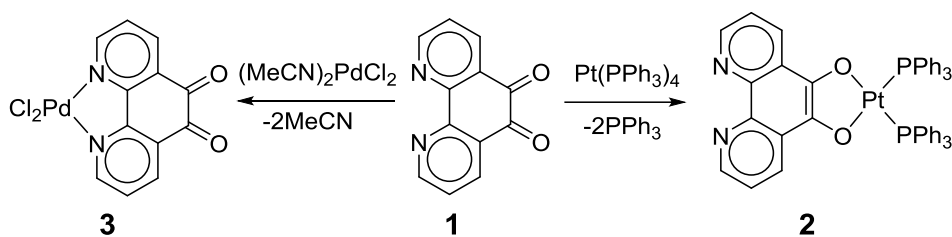

1,10-phenanthroline   1,10-phenanthroline-5,6-dione, **1**
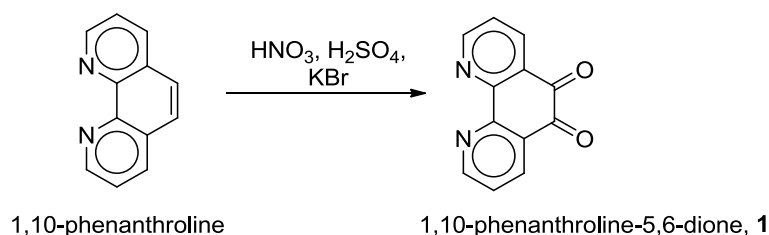
**Scheme 2.** Synthesis of 1,10-phenanthroline-5,6-dione.

Pdon combines two coordination centers. The dioxolene coordination site exhibits typical *o*-quinone properties. A diimine chelating function at the backbone behaves as a 2,2′-bipyridine-like unit. Numerous papers describe diimine coordination mode of pdon ligand only [16–18]. Concerning to bifunctional ligands bearing two different coordination centers, the crucial problem is a separate manipulation by binding of the metal ions with each chelating site.

The coordination bifunctionality of 1,10-phenanthroline-5,6-dione was first shown by Balch in 1975 [19]. Depending on the nature of attacking metal fragment, the resulting product will be NN- or OO-coordinated (Scheme 3). Oxidative addition of the low-valent $Pt(PPh_3)_4$, to the dioxolene site yields to formation of catecholate complex **2**, while $(MeCN)_2PdCl_2$ selectively reacts towards the N-donor center with generation of **3**.

Both mononuclear complexes **2** and **3** bear vacant coordination sites, and could be regarded as either "benzoquinone equivalent" (for complexes (N,N'-pdon) ML_n) or "bipyridine equivalent" (for complexes (O,O'-pdon) ML_n), respectively. Binuclear complex **4** containing both occupied diimine and dioxolene coordination site was described later (Scheme 4) [20].

Scheme 3. Coordination bifunctionality of 1,10-phenanthroline-5,6-dione.
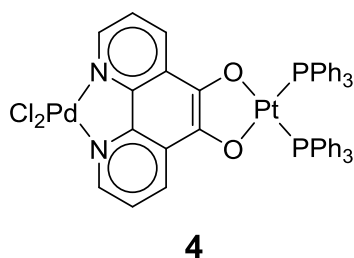
Scheme 4. Binuclear complex **4**.

X-ray crystallography study showed that both metal centers (Pd(II) at diimine site and Pt(II) at dioxolene site, respectively) are in almost square-planar surrounding, which is typical for such complexes. A stacking motif was found for this complex in the crystal lattice: the molecules in stack are parallel to each other, and interplanar distance is 3.29 Å. Moreover, the fragments are rotated relative to each other by approximately 90° in order to provide a short distance between donor and acceptor regions of the adjacent molecules as well as to reduce a steric contact between PPh$_3$ ligands (Figure 1). The stacking motif in a crystal phase was not observed in case of (PPh$_3$)$_2$Pt(O,O'-pdon-N,N')Ru(PPh$_3$)$_2$Cl$_2$ binuclear complex where a bulkier metallofragment is coordinated at the diimine site.
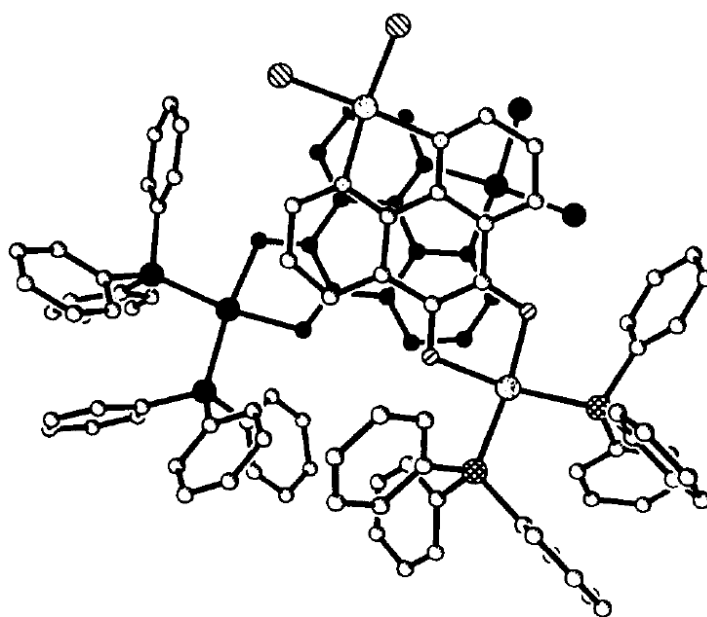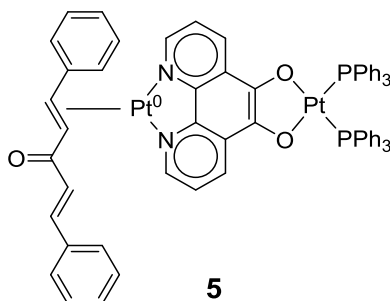

Figure 1. Intermolecular pairing of molecules **4** in solid state. Reprinted with permission from *Inorg. Chem.* **1991**, *30*, 2895–2899. Copyright (1991) ACS.

A reaction of "bipyridine equivalent" (*O,O'*-pdon)Pt(PPh₃)₂ (**2**) with Pt₂dba₃ (dba—dibenzylideneacetone) results in coordination of the platinum (0) at the diimine site to give binuclear complex **5** (Scheme 5).


Scheme 5. Platinum complex **5**.

In the reactions with *o*-quinones this binuclear adduct behaves similar to (bpy)Pt(dba) giving corresponding catecholate complexes [20]. Thus, an interaction of **5** with 3,5-di-*tert*-butyl-*o*-benzoquinone yields to catecholate adduct **6** (Scheme 6).
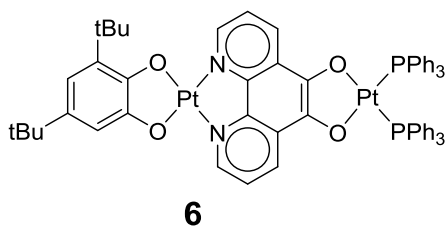
Scheme 6. Binuclear complex **6**.

Electrochemical study of 1,10-phenanthroline-5,6-dione and its complexes showed that introduction of the diimine function made the *o*-quinone unit a more powerful oxidant. Two one-electron peaks corresponding to the *o*-quinone-*o*-semiquinone and *o*-semiquinone-catecholate transformations are observed in acetonitrile at −0.45 V and −1.25 V vs. SCE, respectively [21]. At the same conditions 9,10-phenanthrenequinone reduces at −0.64 V and −1.22 V. Moreover, coordination of a metal ion at the diimine site also significantly affects the electrochemical properties of the *o*-quinone unit, increasing the oxidation ability. In a range of complexes [M(*N,N'*-pdon)₃](PF₆)₂ (M = Co, Ru, Fe), the values of the first reduction potential are shifted from −0.45 V to −0.11 V, −0.13 V and −0.18 V, respectively. Very similar results were observed by Winpenny et al. for [M(*N,N'*-pdon)]Cl₂ (M = Pd, Pt): the dioxolene site reduction processes were found to move to more positive potentials on coordination to a metal center to achieve −0.16 V and −0.12 V for Pd and Pt derivatives respectively [22]. The reduction process at the diimine site in pdon was not observed up to −2.0 V.

Besides of catecholate coordination, there is a possibility of dicarbonyl binding of dioxolene site of pdon at the metal ion. In this case, the dioxolene site exists in an *o*-quinone form as a neutral chelating ligand. Since the Lewis basicity of the diimine site is greater than that of dioxolene site, the Lewis acids in a ratio 1:1 with pdon form mononuclear diimine adducts at the first stage. Dioxolene site becomes involved in binding only when an excess of the Lewis acid is present in the reaction mixture (Scheme 7) [23].
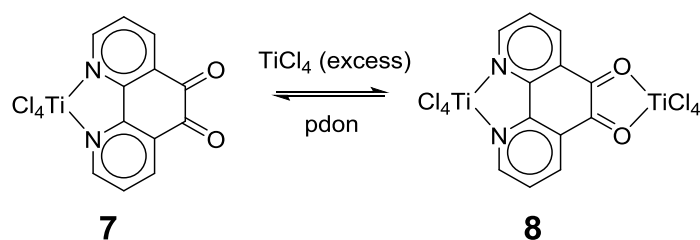
Scheme 7. Synthesis of binuclear Ti complex of pdon.

It was established that the basicity of the diimine unit in pdon is significantly enlarged when a metal is coordinated to the dioxolene site. This is due to the electron donation from the catecholate unit being occupied with a metal ion [24]. Any modification of the surrounding at one coordination site on the bifunctional ligand affects the properties of the remote coordination site. So that the order of priority in the binding of different coordination sites at such bifunctional ligands is essential. When employing the proper synthetic strategy, one can manipulate the selectivity for direction of the metal ion coordination and therefore to avoid undesirable products.

Reduced form of pdon 1,10-phenanthroline-5,6-diol (pdol, **9**) can also act as a precursor for metal complexes. The reaction of **9** with the corresponding metal halide in presence of base was used for synthesis of (tbbpy)Pt(*O,O'*-pdon) (**10**, tbbpy-di-*tert*-butylbipyridine) (Scheme 8) [25].
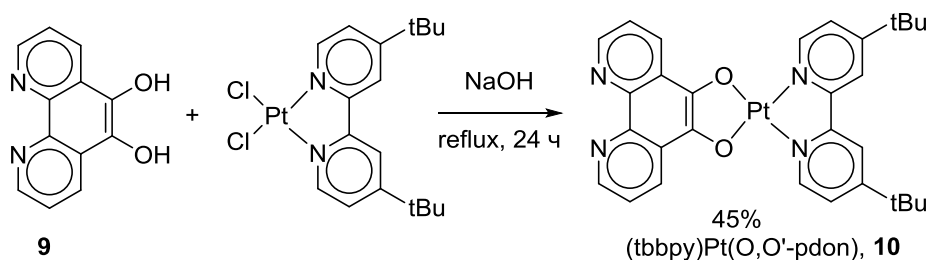

**Scheme 8.** Synthesis of complex **10**.

Combination of two dissimilar coordination sites in one molecule provides an opportunity to use this ligand as a building block in the construction of chain-like or network structures. A series of polynuclear complexes of platinum, as well as heteronuclear Pt-Ru derivatives, were obtained using the step-by-step assembly strategy starting from catecholate (tbbpy)Pt(*O,O'*-pdon) [25]. The initial complex **10**, being a "bipyridine equivalent", interacts with Pt(PhCN)$_2$Cl$_2$ and then with pdol. The resulting adduct **12** is treated with Ru(tbbpy)$_2$Cl$_2$ to give trinuclear species **13** (Scheme 9).

Pampaloni et al. also reported the design of multinuclear systems using the pdon ligand as a building block. A reactivity of the dioxolene and diimine coordination sites towards binding of transition metal ions was studied [23,26–28].

It was shown that, depending on the nature of the metallofragment Cp$_2$M(CO)$_2$, the reaction with pdon proceeds towards the dioxolene site to give semiquinonate (M = Ti) or catecholate (M = Zr, V) species. The oxidation state of the metal ion in Cp$_2$M(*O,O'*-SQ-pdon) was described as +3 in case of Ti and +4 for Zr and V, respectively (Scheme 10) [23].
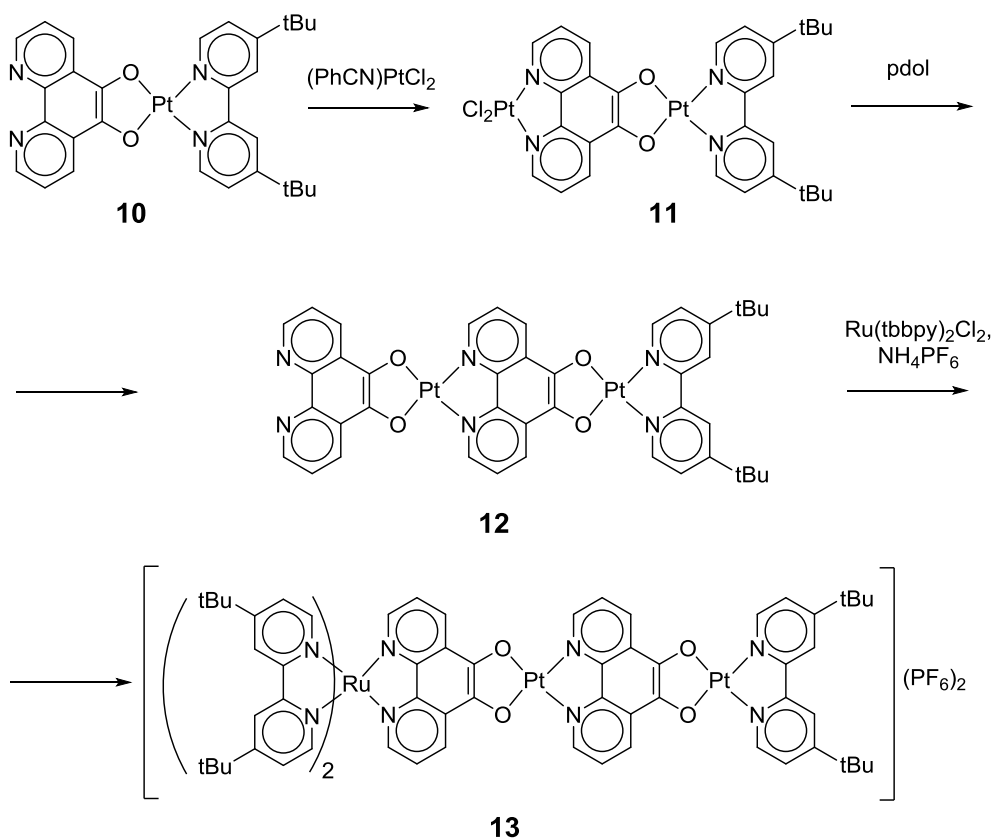
Scheme 9. Generation of trinuclear complex **13** by step-by-step assembly.
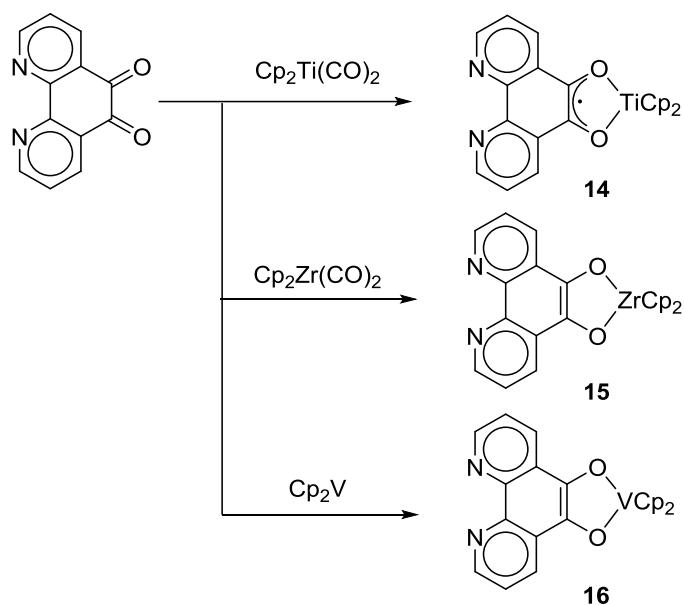
Scheme 10. Oxidative addition of Ti, Zr and V metallofragments to *o*-quinone site.

Cr(CO)$_6$ and Mo(CO)$_6$ react with pdon towards the dioxolene site to give corresponding tris(*o*-semiquinonate) complexes [27]. Reaction of pdon with bis(arene)titanium and vanadium complexes also proceeds as an oxidative addition to the dioxolene site. The mixed-valent complexes M^{IV}(*O*,*O'*-SQ-pdon)$_2$(*O*,*O'*-pdon) (M = V (**17**), Ti (**18**)) were formed at stoichiometry 1:3 of the initial

reagents (Scheme 11) [26]. A comparison of these complexes with 9,10-phenanthrenequinone (phen-Q) structure analogues is worth mentioning: the titanium derivatives indicate a mixed-valent redox state of the dioxolene ligands both in case of pdon and phen-Q, whereas vanadium adduct with phen-Q exhibits semiquinonate state for all three dioxolene ligands. These data correlate well with the electrochemical properties of pdon and phen-Q: the oxidation capacity of 1,10-phenanthroline-5,6-dione is higher than that of 9,10-phenanthrenequinone.

$M^{IV}(O, O'\text{-SQ-pdon})_2(O,O'\text{-pdon})$
M = V (**17**), Ti (**18**)
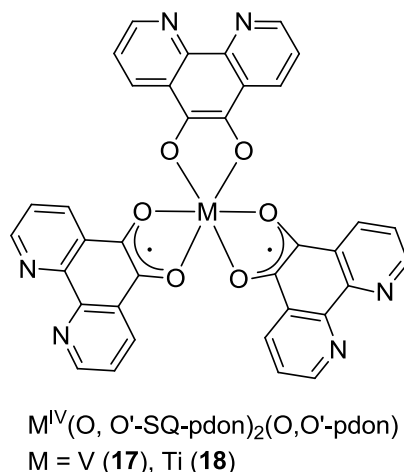
**Scheme 11.** Mixed-valent complexes of vanadium (**18**) and titanium (**19**).

Chromium tris-(pdon) semiquinonate derivative **19** was used as a starting reagent for the syntheses of heteropolynuclear metal complexes. Free diimine unit in **19** interacts with the Lewis acids ($TiCl_2(THF)_2$, $TiCl_4$, $ZrCl_4$, $HfCl_4$, $FeCl_2(THF)_{1.5}$, $CoCl_2$ and $NiBr_2(DME)$) leading to the corresponding tetranuclear species [24,28]. Step-by-step assembling of dendrimer-like structure from $Cr(O,O'\text{-SQ-pdon})_3$ consistently treated with $FeCl_2(THF)_{1.5}$ and pdon were also reported (Scheme 12) [27].

It seems fascinating that the preparation of such heteronuclear species was realized, since it shows the coordination capabilities of the ligand. However, it should be noted that the evidence for the formation of these compounds is insufficient, since the authors rely only on the data of spectroscopic studies.

There are also some examples of lanthanide ions coordination on pdon. It was shown that tris-(β-diketonate) lanthanide (III) complexes attack the diimine site to give corresponding eight-coordinated species. Some of them exhibit luminescent properties. The use of 1,10-phenanthroline-5,6-dione as a neutral ligand in such systems is efficient for several reasons: (i) polynuclear aromatic structure is a chromophore unit, so it can be used as an organic antenna for the sensitization of specific luminescence on lanthanide ion; (ii) coordination of d-metals on the dioxolene center makes possible tuning of the parameters of sensitization.

The complexes $Pt(O,O'\text{-pdon-}N,N')Ln(tta)_3$ (tta—thenoyltrifluoroacetonate, Ln = La (**21**), Gd (**22**), Nd (**23**), Er (**24**), Yb (**25**)) were obtained (Scheme 13) [29,30].

Excitation of **23**–**25** at 520 nm leads to luminescence in the near-IR region both in solution and in the solid state. The platinum metal center at a ligand backbone was found to be photosensitive at this wavelength, so it acts as "antenna" [29,30].
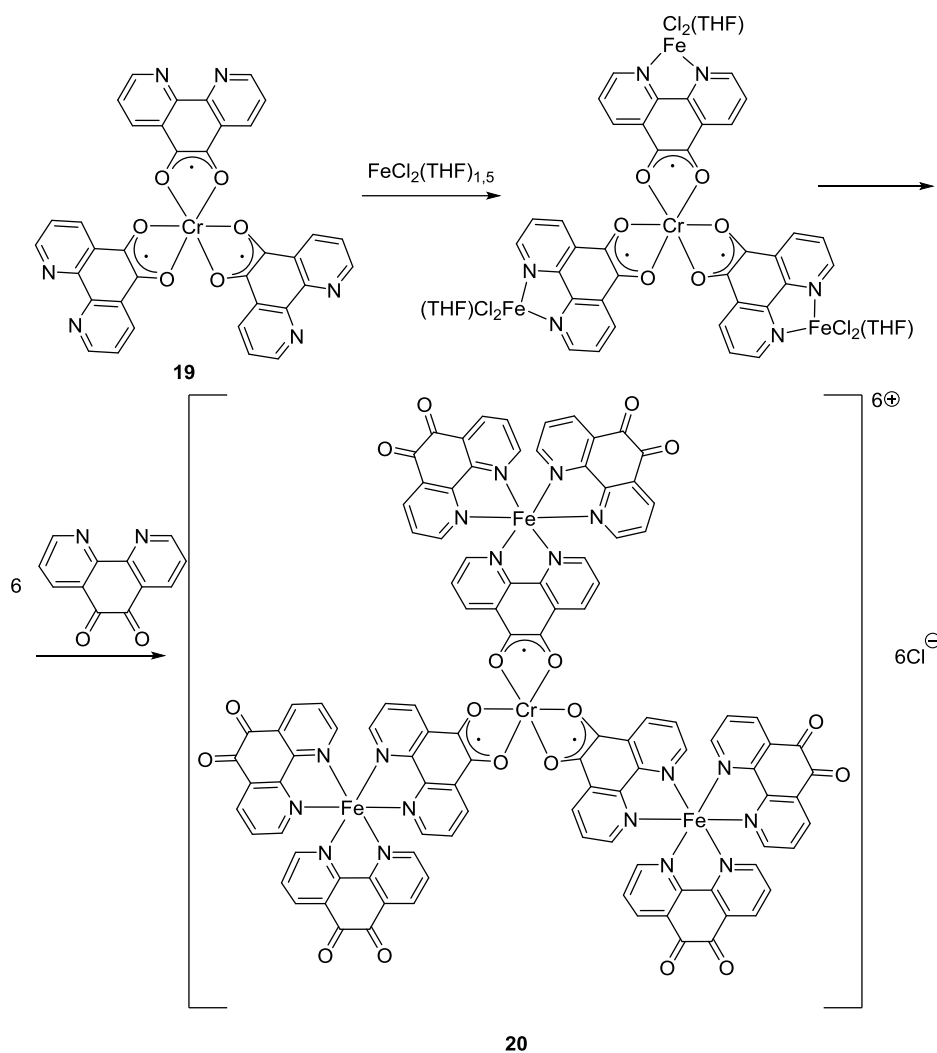
Scheme 12. Generation of dendrimer-like structure with pdon as building blocks.

Ln = La (**21**), Gd (**22**), Nd (**23**), Er (**24**), Yb (**25**)
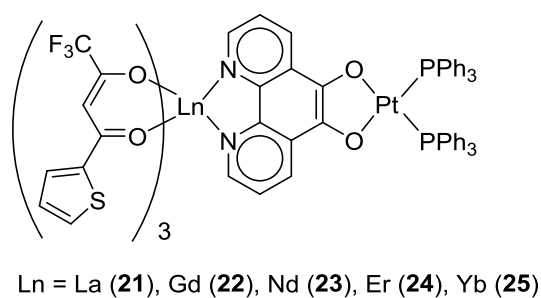
Scheme 13. Tris-(β-diketonate) lanthanide (III) complexes with pdon ligand.

2.2. Bifunctional Catechols, Containing Schiff-Bases

A series of bifunctional redox-active chelating ligands were derived from diaminocatechols. Bifunctional catechols, containing Schiff-bases, were synthesized via condensation of diaminocatechols with 2-pyridinecarboxaldehyde, salicylic aldehyde etc.

In 1993, Coucouvanis et al. proposed a concept of "metal complexes as ligands" [31]. Catechol H_4ETC, annelated with tetraazacyclotetradeca-7,12-dienyl macrocycle, comprises the redox-active catecholate site and N_4-tetradentate coordination center. Several synthetic approaches

resulting in metallocatecholates have been developed. The most versatile one is the condensation of 4,5-diaminoveratrol with 2,2′-(ethane-1,2-diyl-imino)bis(5-methyl-benzaldehyde) in presence of M(OAc)$_2$ (M = Ni (**26**), Co (**27**)) followed by deprotection of catechol function (Scheme 14) [31].
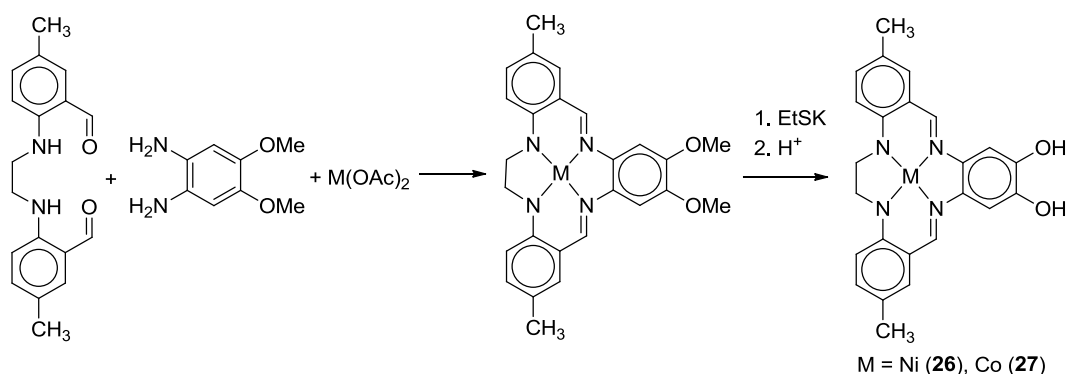
Scheme 14. Synthesis of complexes **26** and **27**.

Dioxolene site of complex could be oxidized to **28** by the ferricinium cation [31]. Crystallography study of the resulting protonated semiquinonate species **28** shows a dimer structure due to hydrogen bonding (Scheme 15).
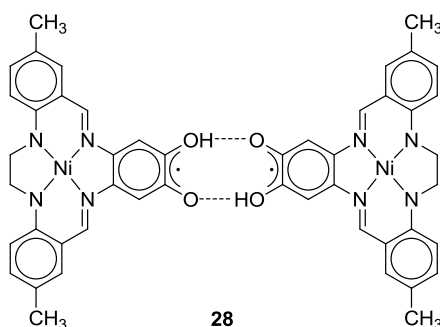
**Scheme 15.** Dimeric structure of species **28**.

Temperature dependence study of the magnetic susceptibility of this dimer reveals antiferromagnetic exchange interactions: the effective magnetic moment is 2.08 μB at 300 K. In contrast, solutions of **28** in DMF and DMSO are diamagnetic and display a narrow ^{1}H-NMR spectrum. It was explained by an electron-proton exchange dynamics in solution leading to formation of catechol-quinone pair.

Treatment of **26** and **27** with *t*Bu$_4$NOH or KOMe in presence of [(DMF)$_3$Mo$_2$O$_2$S$_2$–(S$_2$)] results in heterometallic compounds **29** and **30**. Dimer species **31** and **32** containing Mo–Mo bridge were obtained in the reaction of **26** or **27** with [(DMF)$_3$Mo$_2$O$_2$S$_2$(DMF)$_3$] (Scheme 16) [32].

Jonasdottir et al. reported the synthesis of trinuclear complex **33** where two NiETC moieties are bridged by copper (II) ion (Scheme 17) [33].
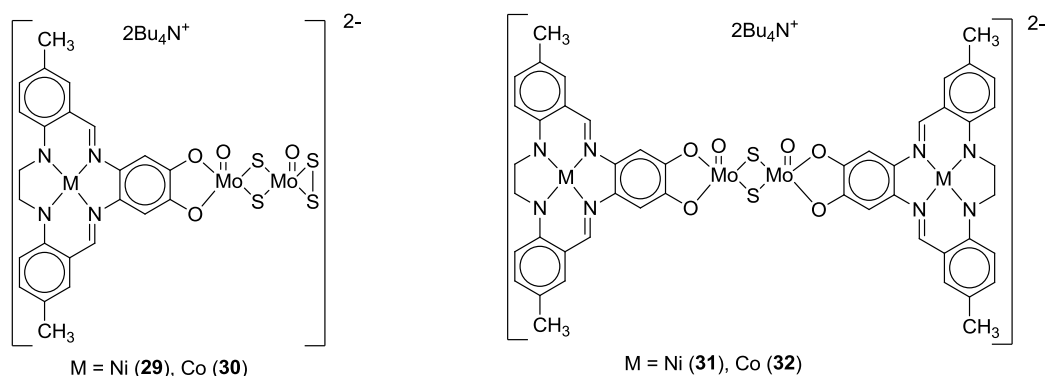
Scheme 16. Heterometallic derivatives **29**–**32**.
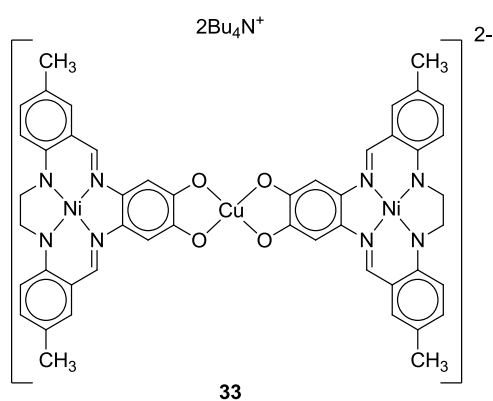
Scheme 17. Trinuclear Ni-Cu-Ni complex **33.**

A family of OO~NN ligands is also presented by bifunctional SALPHEN–catechols that are synthesized by the condensation of 4,5-diaminocatechol with salicylic aldehydes (Scheme 18) [34,35].
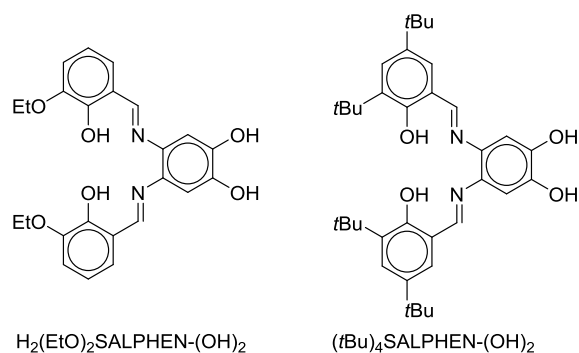
Scheme 18. Bifunctional SALPHEN–catechols.

Malinak et al. developed the procedure for selective preparation of the dimer catecholate adduct $(Bu_4N)_2[Mo_2O_5[H_2(EtO)_2SALPHEN–(O)_2]_2$ **34** (Scheme 19) [34]. Treatment of its vacant SALPHEN sites with $M(OAc)_2$ yields to the corresponding heteronuclear complexes (M = Cu (**35**), Ni (**36**), Co (**37**), Fe (**38**), Mn (**39**)).
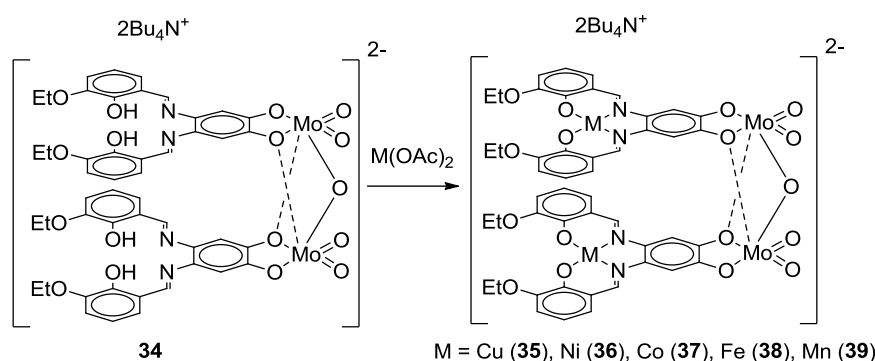
Scheme 19. M-Mo-Mo-M complexes.

Tetranuclear complexes **35** and **36** were characterized structurally; their molecules have a pocket-like structure so that the SALPHEN ligand planes in dimer are almost parallel to each other (Figure 2).
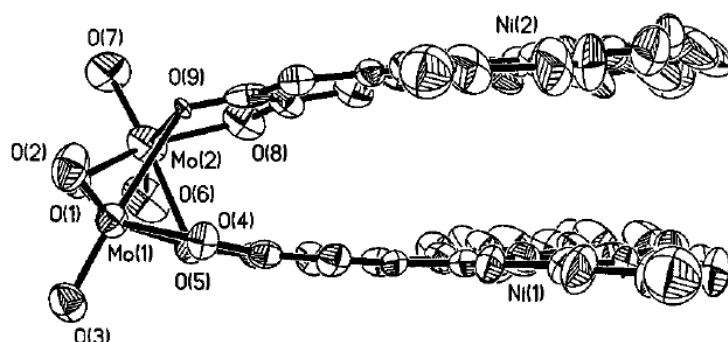

Figure 2. ORTEP plot of complex **36** anion. Reprinted with permission from *Inorg. Chem.* **1996**, *35*, 4810–4811. Copyright (1996) American Chemical Society.

A curious feature of pocket-opening was found for complex **35**. The Cu–Cu bond length in dimer **35** is 4.110 A. This distance can be changed by adding a mixture of pyridine and pyridinium cation into solution: the neutral pyridine molecule coordinates on the molybdenum ion, while pyridinium cation forms hydrogen bonds with the vacant electron pairs of catecholate oxygen. Due to the rearrangement of coordination spheres, valence angle Mo–O–Mo as well as the distances Mo–Mo and Cu–Cu increase, and the pocket between the SALPHEN fragments of **35** is opened (Scheme 20) [34].
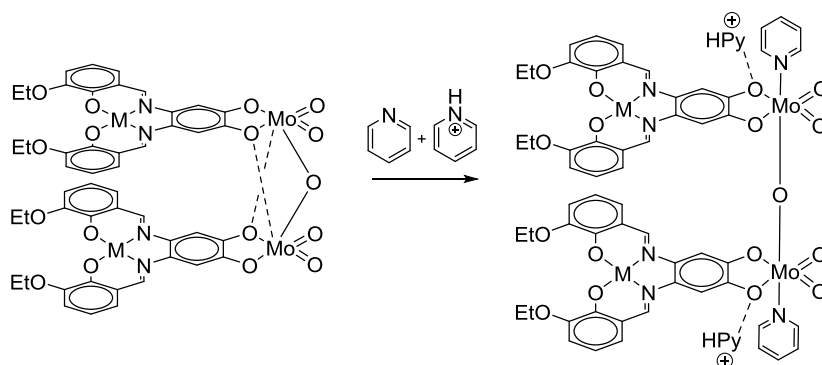

Scheme 20. Activation of pocket-like Mo_2O_5-bridged system.

Another interesting effect was found for iron complex **38**. It was shown that the dimer SALPHEN–complexes of iron (II) interact with dioxygen or sulfur to form inner Fe–X–Fe (X = O, S) bonds, so that a SALPHEN pocket becomes locked. Complexes with bridging oxygen (**40**) and sulfur (**41**) atoms were isolated (Scheme 21) [35].
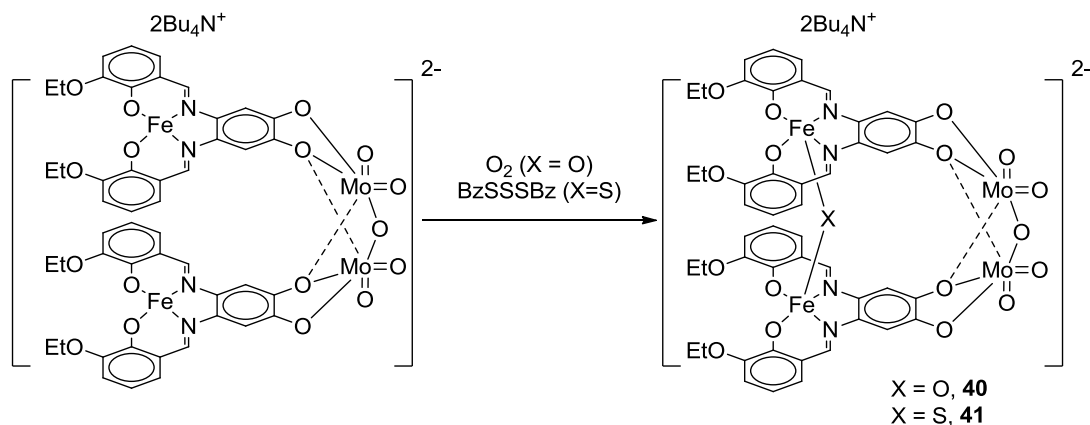
Scheme 21. Intramolecular bridging of Fe atoms with sulfur and oxygen atoms.

The more sterically hindered (*t*Bu)$_4$SALPHEN–(OH)$_2$ forms mixed-ligand catecholate complexes **43**–**46**. SALPHEN–catechol replaces only one catecholate fragment (3,5DBCat) in adduct **42** (Scheme 22). The formation of a homoligand dimer adduct is unfavorable due to the steric reasons [35].
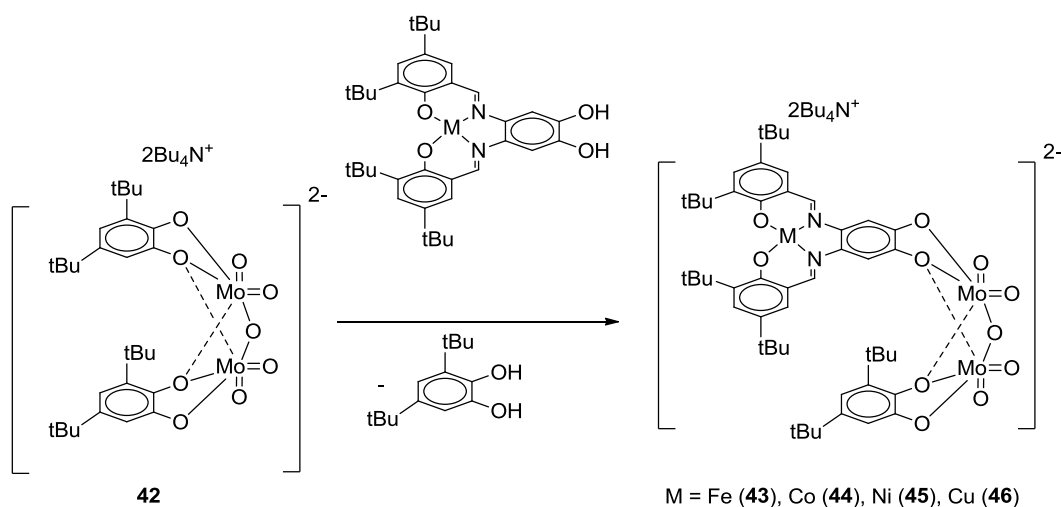
Scheme 22. The formation of mixed-ligand molybdenium complexes.

A series of Zr heterobinuclear complexes **51**–**53** were reported for SALPHEN ligands (Scheme 23). Some of them have been investigated as catalysts for polymerization of olefins [36].
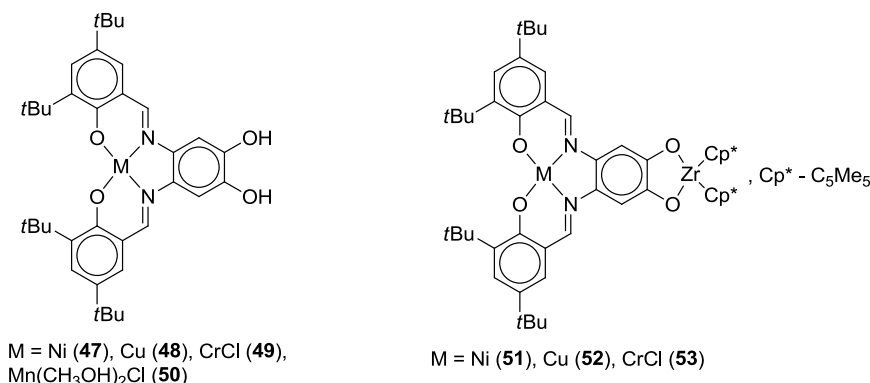
**Scheme 23.** Mono- and binuclear complexes **47–53**.

Weber et al. reported OO~NN ligand that was prepared via condensation reaction of 4,5-diaminocatechol with keto-enol-ether [37–39]. A series of Fe (II) complexes **54–60** bound at the diimine site of this ligand were studied (Scheme 24). Some interesting effects including an influence of intramolecular hydrogen bonding on the magnetic behavior of these complexes were found. There are also very promising results concerning to construction of 1D polymeric chains using bidentate pyridine auxiliary ligands as a bridge. Some of these coordination polymers were found to exhibit spin-crossover phenomena.
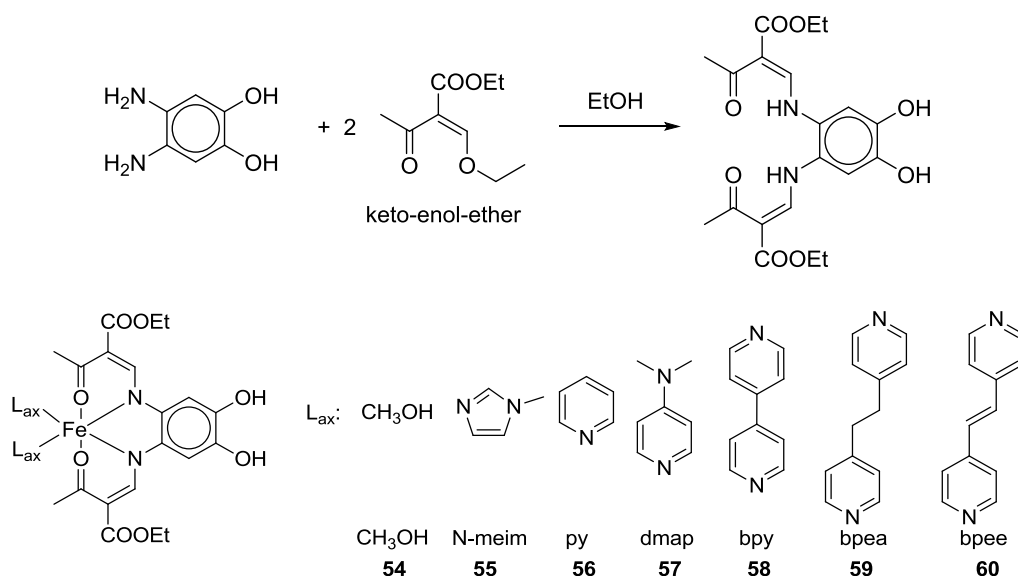
Scheme 24. A series of Fe (II) complexes with keto–enol–ether bifunctional ligand.

Trinuclear complexes [Cu$_3$L$_2$](Bu$_4$N) (**61**) and [V(O)Cu$_2$L$_2$](Bu$_4$N) (**62**) have been studied in order to understand the mechanisms of exchange interactions between magnetic centers in a planar linear coordination polymeric chain (Scheme 25). It was shown that depending on the symmetry of the orbitals of the central metal ion exchange interactions between terminal Cu(II) centers may be antiferromagnetic or ferromagnetic as for **61** and **62**, respectively [40].

M = Cu (**61**), V(O) (**62**)
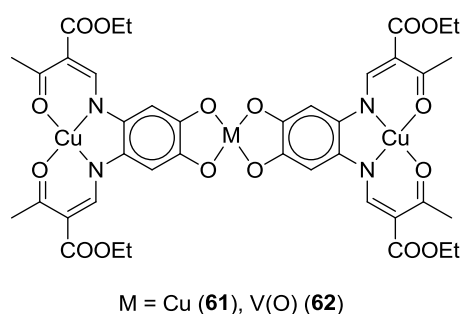
Scheme 25. Trinuclear complexes with keto–enol–ether bifunctional ligand.

Investigation of complexes containing NN~OO bifunctional chelating ligands indicates their potential for future technological applications. Two different coordination sites facilitate construction of ordered structures. A redox activity of the dioxolene site is useful in managing the geometry or other parameters of complexes. At the same time, redox transformations at diimine site in such bifunctional ligands are not accessible at ordinary conditions. Introduction of dithiolene site instead of diimine one provides an opportunity for the interplay between redox abilities of two sites.

3. SS~OO Systems

There are a limited number of redox-active benzenoid ligands combining dioxolene and dithiolene sites. A synthetic procedure for the preparation of the 4,5-dimercaptocatechol **63** was first reported by Coucouvanis et al. (Scheme 26) [41].
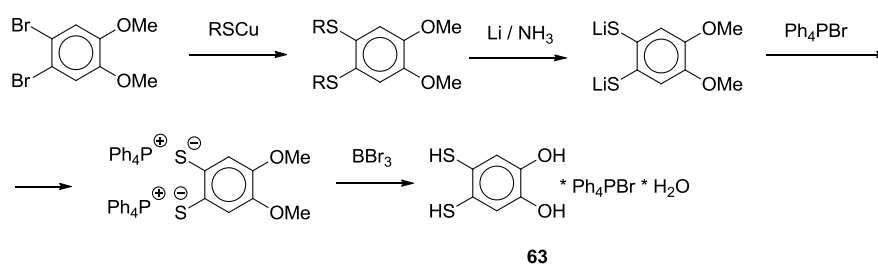
Scheme 26. Synthesis of 4,5-dimercaptocatechol.

All reported complexes containing this ligand reveal a dithiolene mode of coordination of the metal ion. A series of bis(dithiolate) complexes were synthesized. According to the structural parameters the metal ion in $[M(DtCat_2)^-]$ $[Ph_4P^+]$ adopts M^{3+} state both in case of M = Cu (**64**) and M = Ni (**65**) (Scheme 27).

M = Cu (**64**), Ni (**65**)
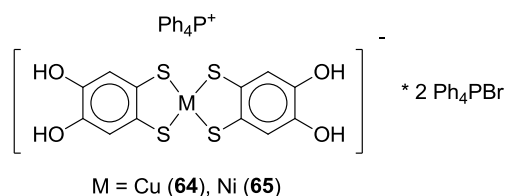
Scheme 27. Bis(dithiolate) derivatives of 4,5-dimercaptocatechol $[M(DtCat_2)^-]$ $[Ph_4P^+]$.

Hydroxyl groups in **64** and **65** could be selectively oxidized by the molecular oxygen leading to the corresponding bis(dithiolates) **66** and **67**, those contain non-coordinated *o*-quinone sites at the termini (Scheme 28).

$$2 \; Ph_4P^+ \qquad 2-$$

M = Cu (**66**), Ni (**67**)
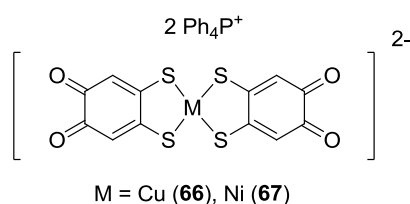
Scheme 28. Bis(dithiolates) with non-coordinated *o*-quinone moiety.

Unfortunately, the reactivity of metal ions towards binding at dioxolene site of the molecule has not been studied yet.

Recently, we reported the substituted analogue of SS~OO bifunctional redox active chelating ligand. It was found that the decarbonylation of 4,7-di-*tert*-butyl-1,3-benzodithiole-2,5,6-trione yields the sterically-hindered *o*-quinone, annelated with dithiete (**68**) (Scheme 29) [42].
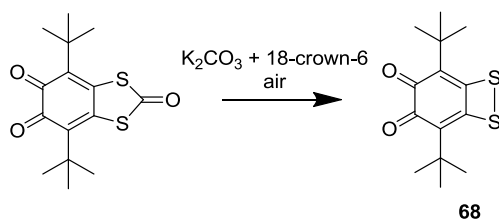
Scheme 29. Synthesis of *o*-quinone, annelated with dithiete cycle.

It is a unique bifunctional ligand, containing two different redox-active chelating chalcogen coordination centers. Since dithiete is an electronic analogue of 1,2-dithiocarbonyl function, the dithiolene and dioxolene sites in the ligand are in the same oxidation state. The different properties of sulfur and oxygen create an opportunity for manipulation of the direction of metal ion binding during the reaction of oxidative addition. This species presents a unique chance to compare an activity of dithiolene and dioxolene sites being in the same steric surrounding and under the same conditions in different reactions with metals.

It was shown that the direction of an oxidative addition depends on the nature of metallofragment. Treatment of the ligand with one-electron reducing agents such as Li, Na, K, Tl, Cu (in presence of PPh$_3$), Mn$_2$(CO)$_{10}$ yields in *o*-semiquinonate species. Alkali metal *o*-semiquinonates can undergo further reduction to give corresponding catecholates. According to the EPR spectroscopy data vacant dithiolate site in the manganese semiquinonate adduct **69** can be also involved into the oxidative addition process. Interaction of **68** with an excess of Mn$_2$(CO)$_{10}$ results in subsequent formation of semiquinonate **69** and then the trinuclear species **70** (Scheme 30) [42]. Mononuclear semiquinonate **69** has a sextet lines EPR spectrum in toluene due to splitting of the unpaired electron on the ^{55}Mn nucleus (Figure 3a). A multiplet spectrum that arises upon further reduction of **69** with Mn$_2$(CO)$_{10}$ was attributed to the trinuclear species **70**. The unpaired electron in **70** interacts with one manganese nucleus at the dioxolene site and with two equivalent manganese nuclei at the dithiolene unit (Figure 3c). The hyperfine splitting (HFS) constant values are 6.80 G and 1.39 G respectively.
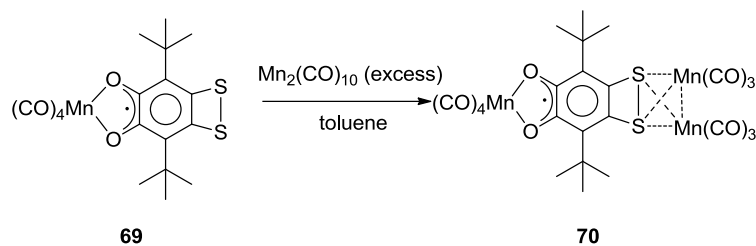
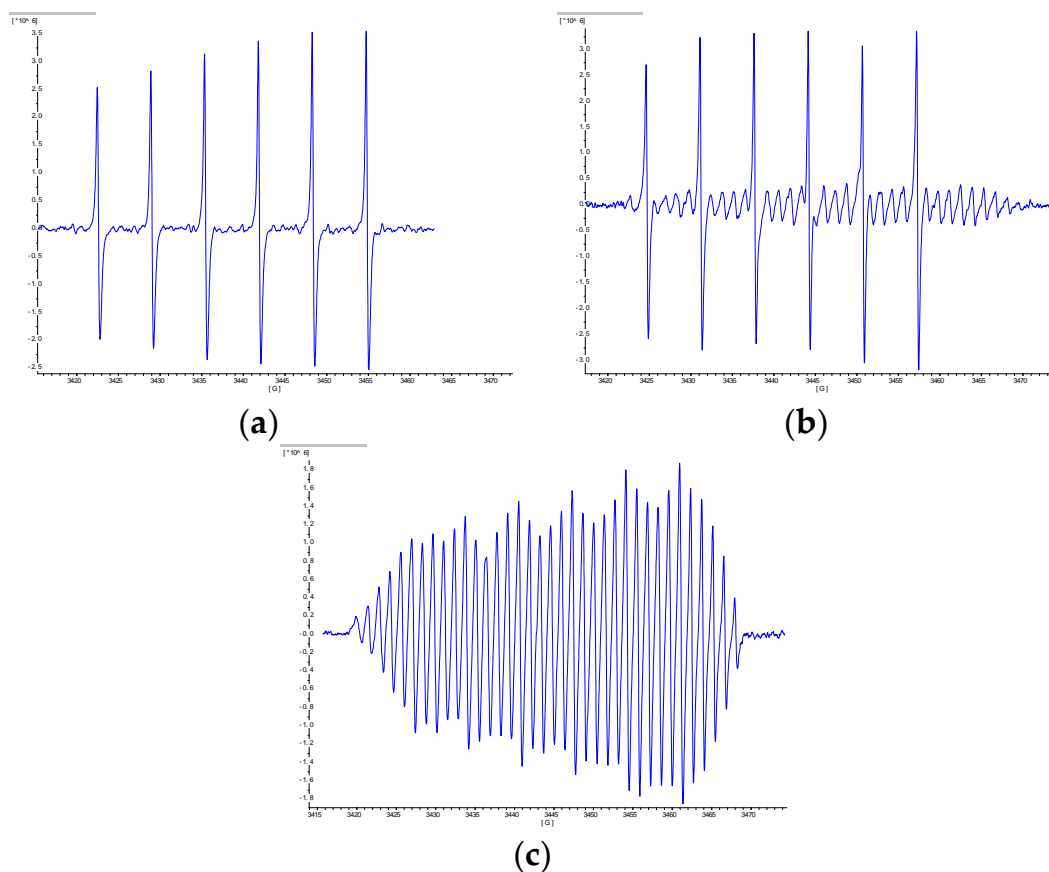**Scheme 30.** The formation of trinuclear species **70**.

Figure 3. Evolution of the EPR spectrum of the mixture of *o*-quinone **68** and $Mn_2(CO)_{10}$ in toluene upon irradiation with halogen lamp. (**a**) 30 s later, the signal corresponds to the mononuclear adduct **69**; (**b**) 10 min later, the observed signal is a superposition of signals from paramagnetic species **69** and **70**; (**c**) 20 min later, the signal is attributed to the trinuclear adduct **70**.

Reaction of **68** with two-electron reducing agents results in catecholate or dithiolate derivatives depending on the Lewis acidity of the metal ion. Binding at the dithiolate coordination site is preferable for the soft Lewis acids and vice versa. Group 10 zero-valent metal tetrakis (triphenylphosphine) complexes $M(PPh_3)_4$ (M = Pd, Pt) selectively react towards dithiolene site of the ligand **68** with formation of **71** and **72** mononuclear adducts (Scheme 31) [43].
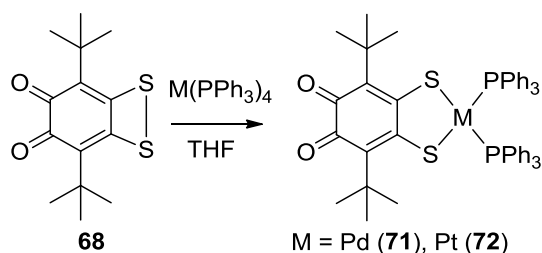
Scheme 31. Regioselective oxidative addition of $M(PPh_3)_4$ (M = Pd, Pt) towards dithiolene site. (Reproduced from *Dalton Trans.* **2016**, *45*, 7400–7405. Copyright (2006) Royal Society of Chemistry).

According to the cyclic voltammetry data, coordination of a metal fragment on the dithiolene site significantly decreases the first reduction potential of free dioxolene site from -0.42 V (**68**) to -0.90 V (**71**) and -0.80 V (**72**). Nevertheless, such mononuclear complex still might be regarded as an *o*-quinone equivalent and can be reduced by many one-electron agents to give corresponding heterobimetallic complexes (Scheme 32) [43].
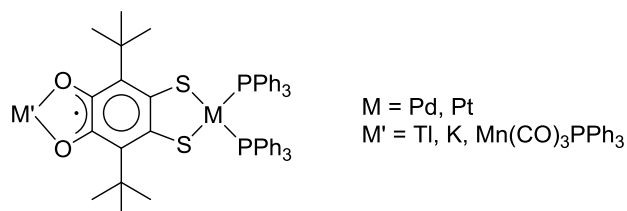
Scheme 32. Heterobimetallic semiquinonate adducts.

A diversity in the oxidation addition of a metal to the ligand **68** was found in case of Pd(dppe) metallofragment. Both dithiolate **73** and catecholate **74** isomers were isolated and characterized by NMR, IR-spectroscopy and X-ray analysis (Scheme 33) [44].
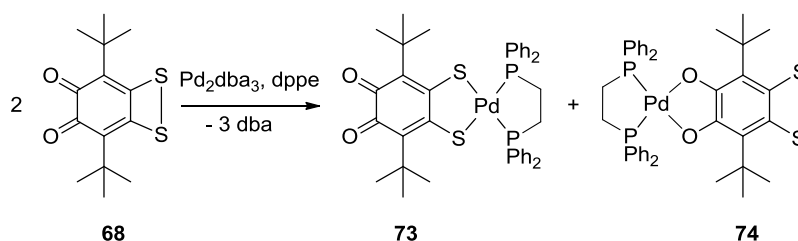
Scheme 33. The formation of two regioisomers **73** and **74**. Reproduced from *Dalton Trans.* **2017**, *46*, 16783–16786. Copyright (2017) Royal Society of Chemistry.

According to DFT calculations the difference in energy between these isomers is rather small. This is the main reason for the diversity in the oxidative addition. The ratio of isomer products in the reaction mixture depends on the method of preparation, solvent polarity, temperature and so on. Nevertheless, the catecholate species **74** is more stable, so that in solution it slowly isomerizes into the dithiolate one (Scheme 34). This is the first example of regioisomerism in coordination chemistry [44].
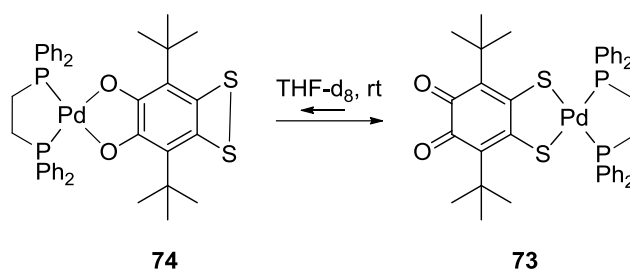
Scheme 34. Isomerization of **74** to **73**. Reproduced from *Dalton Trans.* **2017**, *46*, 16783–16786. Copyright (2017) Royal Society of Chemistry.

Indeed, the isomers **73** and **74** possess different chemical properties. Mononuclear dithiolate complex **73** as an *o*-quinone equivalent is capable to form heterobinuclear semiquinonates being reduced with alkali metals or other one-electron reducing agents. Catecholate isomer **74** could be oxidized in solution into the corresponding semiquinonate species. The parameters of EPR spectrum of this adduct are highly consistent with those reported for $(PPh_3)_2Pd(3,6-t-Bu-o-benzosemiquinonate)$ [45].

Understanding the mechanisms that regulate the direction of catecholate or dithiolate mode of binding of the metal ion in case of ligand **68** could be useful from the viewpoint of potential application in the stepwise assembling of ordered structures. Such binucleating constructions might be applied as molecular devices. Moreover, the SS~OO system can be regarded as a junction between the bulk metal electrode and a key part of the molecular device, due to affinity of sulfur to noble metals (Scheme 35).
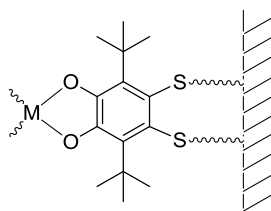

Scheme 35. Potential application of ligand **68** as a junction to a bulk metal.

4. Di-*o*-Quinones Containing Acceptor-Donor-Acceptor Systems

The energy gap between the lowest unoccupied and highest occupied electronic level is an important parameter determining the redox, electronic, optical, and conductive properties of a material. Multistage organic amphoteric redox systems with a small HOMO/LUMO gap (<0.5 eV), are of considerable interest due to their potential applications in molecular electronics and optoelectronics. Consequently, research efforts focused on the design and synthesis of molecular systems composed of strong electron donor (D) and acceptor (A) units. The main principles for constructing low band-gap organic fused compounds were generalized by Perepichka et al. They include (i) tailoring the aromatic/quinoid character of a conjugated system; (ii) its rigidification into a planar conformation; (iii) the alternation of π-donor and π-acceptor fragments in the polymer chain [46]. Decoration of such amphoteric redox systems with chelating coordination sites provides multiple opportunities for construction of ordered structures in a crystal phase using metal ions as nodes.

4.1. Amphoteric Redox Triad Consisting of Two o-Quinone Units Linked by TTF Bridge

An effort to combine in one molecule the units bearing both high-lying HOMO and low-lying LUMO levels resulted in an A-D-A triad system consisting of fused strong donor (TTF) and powerful acceptor (*o*-quinone) moieties [47]. In contrast to many other A-D-A triads the chelating *o*-quinone moieties at the termini of the Q-TTF-Q molecule **75** are capable of binding metal ions (Scheme 36).

Q-TTF-Q, **75**
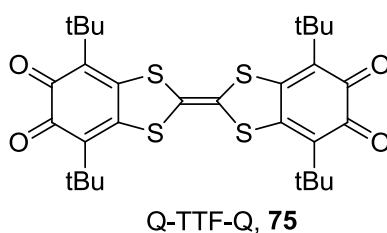
Scheme 36. Redox triad A-D-A consisting of annelated *o*-quinone and TTF units.

The molecule of Q-TTF-Q was assembled from three moieties. Central TTF unit originates from disodium tetrathiooxalate molecule which was linked by an exchange reaction to 3,6-di-*tert*-butyl-4-chloro-*o*-benzoquinone followed by cyclization (Scheme 37).
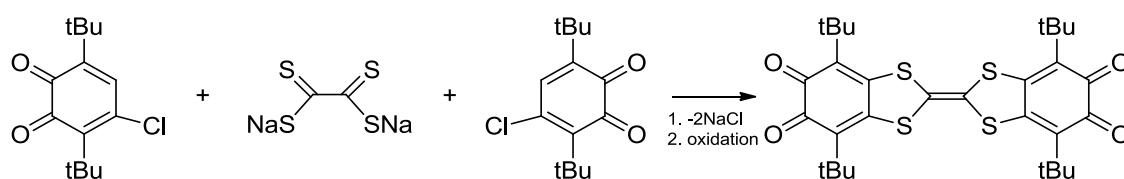
Scheme 37. Synthesis of Q-TTF-Q. Reproduced with permission from *Tetrahedron* **2010**, *66*, 7605–7611. Copyright (2010) Elsevier.

This method was first reported in 2010 and its main advantage is highly effective one-stage process, the only by-product is S-bridged di-*o*-quinone (**76**) (Scheme 38) [47]. The overall preparative yield of Q-TTF-Q is 67%.
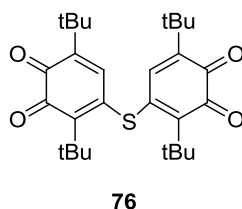

76

Scheme 38. Sulfur bridged di-*o*-quinone **76**.

X-Ray diffraction study reveals a rigid planar structure for A-D-A triad **75**. Despite a fused construction of the molecule, the structural parameters of the constituent units in the triad are typical for *o*-quinone and TTF, respectively. Both *o*-quinone and TTF moieties might be regarded as relatively independent, and, as a consequence, should retain their characteristic properties. A conjugation of donor and acceptor units in one molecule leads to an efficient intramolecular charge transfer. For Q-TTF-Q it manifests in a wide intensive band in the electronic spectrum with a maximum at 564 nm (Figure 4).
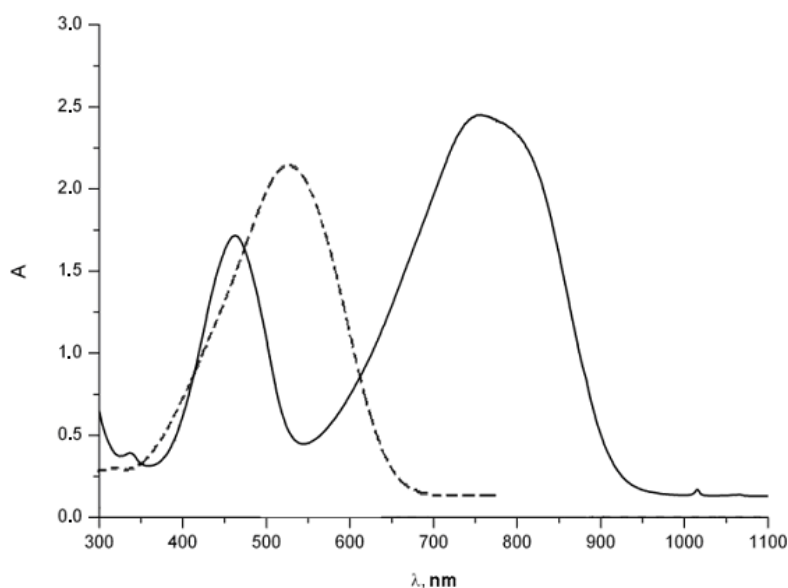
Figure 4. UV/vis spectra of **84** (solid line, c = 2.5×10^{-5} M, 1 cm quartz cell) and **75** (dashed line, c = 1.7×10^{-5} M, 1 cm quartz cell) CH$_2$Cl$_2$.
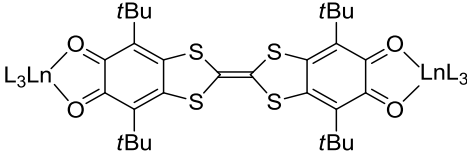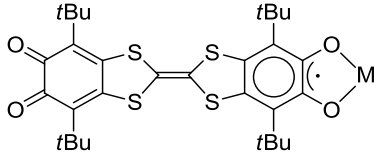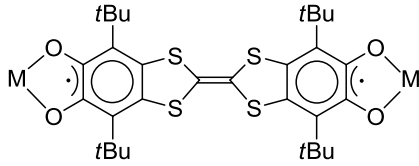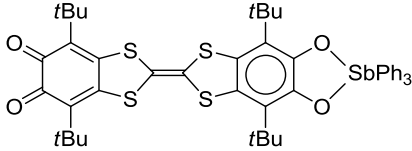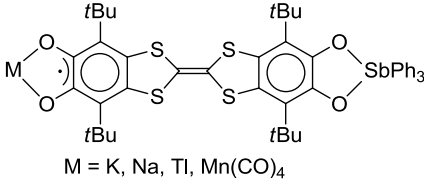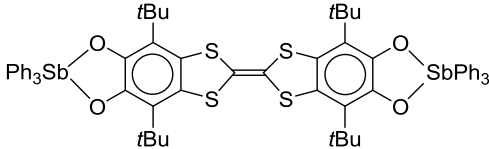
By means of π–π interactions between the adjacent molecules the triad **75** forms stacks in a crystal phase. Each next molecule in the stack is shifted relatively previous one by 5.57 Å in order to provide a short contact between the oxygen atoms of one molecule and sulfur atoms from the adjacent one (Figure 5).

Figure 5. Stacking motif in crystals of Q-TTF-Q. Reproduced with permission from *Tetrahedron* **2010**, *66*, 7605–7611. Copyright (2010) Elsevier.

Q-TTF-Q as a ligand displays various coordination modes. Depending on the intrinsic redox state of the triad as well as a nature of metal ion Q-TTF-Q ligand could be bridging or terminating (Table 1). Both terminating and bridging coordination modes were observed in case of dianion form of the ligand [48,49].

Table 1. Bridging and terminating coordination modes for Q-TTF-Q in different oxidation states.

Redox State	Coordination Mode	
	Bridging	Terminating
0	Ln = Y, Dy, Gd, Yb, Er; L = hfac, tta	-
−1	-	M = K, Na, Tl, Tl(Me)$_2$, Mn(CO)$_4$
−2	M = K, Na, Tl, Tl(Me)$_2$	
−3	M = K, Na, Tl, Mn(CO)$_4$	-
−4		-

According to DFT calculations, performed by Gaussian 03 at the B3LYP/6-31G* level of theory, HOMO in **75** is presumably localized at the TTF unit, whereas LUMO is situated at *o*-quinone moieties. The HOMO–LUMO gap in **75** was estimated to be 2.41 eV. This value is in a good agreement with the electrochemical and spectroscopic data [47].

Electrochemical study showed four one-electron reduction processes for Q-TTF-Q at −0.4, −0.61, −1.04 and −2.56 V, respectively. They were attributed to stepwise reduction of *o*-quinone sites at the termini of the molecule. Electrochemical oxidation of Q-TTF-Q at 1.40 V seems to be two-electron and irreversible (Scheme 39).
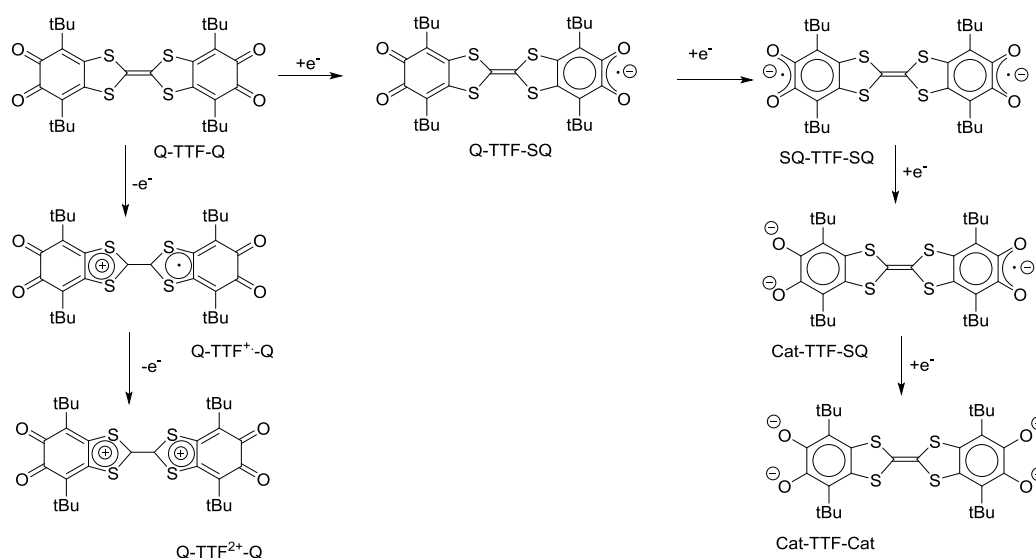
Scheme 39. Electrochemical transformations of Q-TTF-Q species.

EPR spectroscopy investigation indicated very similar behavior upon chemical reduction of the Q-TTF-Q. Being treated with alkali metal, the Q-TTF-Q undergoes four reduction steps, the adducts at first and the third ones are paramagnetic. In contract to the electrochemistry data, an oxidation of Q-TTF-Q with TCNQ indicates an availability of radical-cation state for the Q-TTF-Q. The existence of this species was confirmed by the EPR spectroscopy data [48].

As bis-chelating ligand, Q-TTF-Q can be used for the construction of assembled structures. Chain-like ordering was found for the mononuclear Q-TTF-SQTl(Me)$_2$ **77** adduct in the crystal lattice. Dimetylthallium anion acts as a node linking the ligands into the chain (Figure 6). Notably, the ligand's planes in the chain are parallel to each other. The equatorial positions of each Tl octahedron are occupied with semiquinonate oxygens from one ligand molecule and with *o*-quinone oxygens owned by the adjacent ligand unit. The methyl groups are situated in the apical positions, respectively. All the coordination polymeric chains in the crystal are stretched along one direction [49].
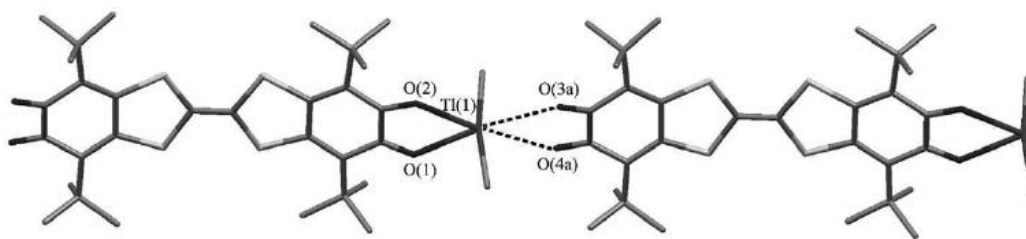
Figure 6. 1 Dimension ordering of **77** species. Reproduced with permission from *Zeitschrift für anorganische und allgemeine Chemie* **2011**, *637*, 232–241. Copyright (2010) John Wiley and Sons.

Magnetic measurements reveal the value of μ_{eff} = 1.74 μB at 300 K for **77**. This is very close to the expected value of 1.73 μB for the spin system with S = 1/2 (doublet state). Such behavior is typical for ordinary mono-*o*-semiquinonato complexes containing one unpaired electron. Below 50 K, the magnetic moment falls probably due to an intermolecular antiferromagnetic exchange.

All studied binuclear metallocomplexes with the Q-TTF-Q ligand in the redox state −2 display a strong antiferromagnetic intraligand exchange. This manifests that the planar TTF linker provides an effective channel for electronic communication between semiquinonate units at the termini.

Q-TTF-Q was found capable of forming binuclear complexes with lanthanides (III) β-diketonates as a neutral ligand. Treatment of Ln(hfac)$_3$·2H$_2$O (hfac—hexafluoroacetylacetonate) with Q-TTF-Q in the ratio 2:1 results in binuclear species Ln$_2$(hfac)$_6$L (Scheme 40) [50,51].
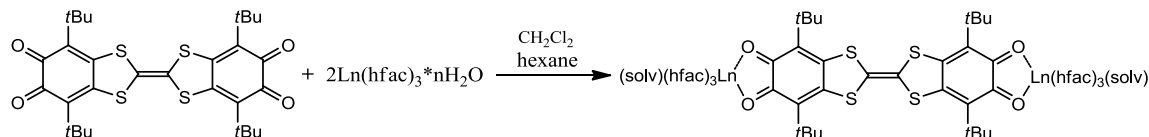
Scheme 40. Complexes of Q-TTF-Q with Ln(hfac)$_3$ (Ln = Dy (**78**), Gd (**79**), Y (**80**), Er (**81**), Yb (**82**)).

Complex **78** with D$_{3h}$ symmetry at the Dy ion behaves as a SMM. This behavior is attributed to a single-ion feature. Obviously, the binuclear complex is regarded as two single-ion magnets linked by an electro-active A-D-A bridge [50].

Highly promising luminescent properties were found for the Yb binuclear complex **82**. The excitation-induced line-shape emissions in the near-infrared spectral range have been assigned to the ytterbium-centered transition. It was established that the antenna-effect sensitization process is favored and proceeds by energy transfer from the singlet CT state of the Q-TTF-Q chromophore. Remarkable that the energy of the charge-transfer donating state is estimated to be 13,585 cm^{-1}, that is, the longest wavelength reported for Yb (III) sensitization [51].

4.2. p-Phenylene Extended Amphoteric Redox Triad

Q-TTF-Q showed promising results concerning to luminescent and magnetic properties. An assembling potential due to the chelating dioxolene functions at the termini also favors continuation of studies of this species as a ligand. Its main disadvantage is relatively high HOMO–LUMO energy separation. There are two opportunities to make it narrower. The first one is to use more withdrawing *o*-quinone in order to reduce the LUMO level. Another one is an introduction of a more donor linker instead of TTF bridge. Among them, the second strategy seems to be more appropriate.

The *p*-phenylene insertion was introduced into the TTF unit in order to decrease the HOMO–LUMO gap in the triad, since the addition of *p*-phenylene spacer in TTF molecule moves first oxidation potential from 0.32 V to −0.05V [52].

The synthesis of the Q-exTTF-Q was performed using a similar approach as that was used for the Q-TTF-Q preparation. Interaction of 4-chloro-3,6-di-*tert*-butyl-1,2-benzoquinone with sodium tetrathioterephtalate resulted in formation of adduct with extended TTF bridge [53].

The triad Q-exTTF-Q was isolated as the diprotonated direduced species **83**. It could be oxidized into the di-*o*-quinone form **84** (Scheme 41). The di-*o*-quinone form was characterized in solution only, all attempts of crystallization failed. Nevertheless, it was shown that the triad Q-exTTF-Q in di-*o*-quinone form is quite stable in dilute solutions, so that being freshly prepared could be used as a starting reagent for further synthesis of complexes.

X-ray diffraction study of the direduced diprotonated form of Q-exTTF-Q **83** reveals a rigid planar structure for the molecule. The geometry parameters surely correspond to zwitter-ionic structure of the molecule. DFT study showed that the singlet biradical is a ground state for the **83**.

Like Q-TTF-Q, the extended triad **83** forms stacks in the crystal lattice (Figure 7). The packing motif is similar: Carbonyl oxygens are located in the immediate vicinity of the sulfur atoms of the adjacent molecule. Minimal distances between sulfur and oxygen atoms in the stack are 3.316 and 3.393 A. These values are comparable with the sum of the van-der-Waals radii (3.32 A).

Indeed, introduction of the *p*-phenylene spacer caused a decrease of the HOMO–LUMO energy separation (1.69 eV), so as to compare with the Q-TTF-Q (2.41 eV). This fact is in a good agreement with the UV–vis spectroscopy data. In electronic spectrum of **84** in CH$_2$Cl$_2$ the band attributed to the intramolecular charge transfer is centered at 757 nm (Figure 4).
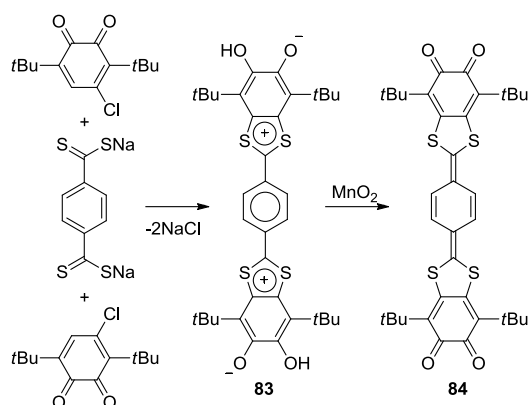
Scheme 41. Synthesis of Q-exTTF-Q and its diprotonated direduced form. Reproduced with permission from *Eur. J. Org. Chem.* **2014**, *2014*, 4571–4576. Copyright (2014) John Wiley and Sons.
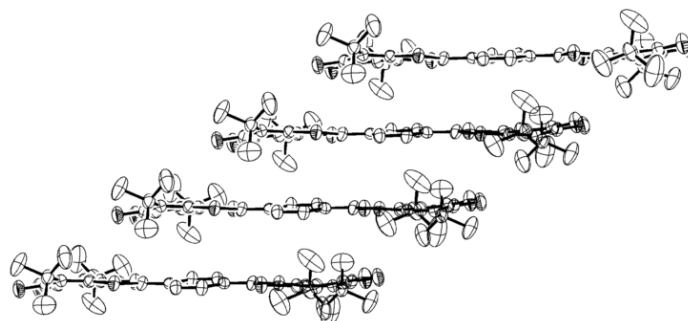
Figure 7. Stacking motif of **83** in crystal phase. Reproduced with permission from *Eur. J. Org. Chem.* **2014**, *2014*, 4571–4576. Copyright (2014) John Wiley and Sons.

Redox properties of the di-*o*-quinone **84** were evaluated in reduction reactions with alkali metals. The chemical behavior of the ligand is identical to that of Q-TTF-Q: reduction of **84** proceeds in four one-electron steps: "di-*o*-quinone"—"*o*-quinone—*o*-semiquinone"—"di-*o*-semiquinone"—" *o*-semiquinone—catecholate" and "dicatecholate" [54]. Reduction of the diprotonated form **83** with copper in presence of 1,2-bis(diphenylphosphino)ethane leads to formation of solvent-separated radical ion pair **85**: Cu(dppe)$_2$$^+$ and ligand in anion-radical state (Scheme 42) [55].
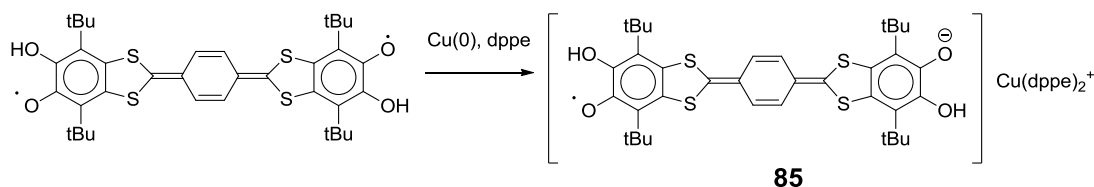
Scheme 42. Reduction of **83** with metal copper.

This species allows estimating the contribution of extended TTF spacer in the mechanism of the electronic communications between semiquinonate rings at the termini of the molecule. EPR spectroscopy reveals for **86** fully symmetric distribution of spin density along the Q-exTTF-Q ligand that indicates the system belongs to class III of Robin–Day classification of mixed valence systems [56], so that, the exTTF linker acts as an effective channel for the electronic communications.

While much remains to be done, we believe that the Q-exTTF-Q is very perspective building block to be used in search of systems exhibiting luminescence and molecular magnetism phenomena.

5. Conclusions

In this review, we have discussed the major advances that have recently been achieved in fields of synthesis and applications of *o*-quinones decorated with additional chelating coordination sites as well as redox-active functions. The authors of this brief review did not grasp the immensity and describe all classes of bifunctional chelating ligands.

We tried to show that coordination capabilities of *o*-quinone-based bifunctional chelating ligands provide good opportunities for the assembling of coordination polymers. In combination with redox activity, this is a very useful perspective from the viewpoint of construction of the molecular devices.

The fragility of many organic-based molecular devices still stands as a major limitation toward their application in real-world electronic devices. From this point of view, *o*-quinone derivatives exhibit quite high stability. Further synthetic attempts will discover more novelty in the future.

Conflicts of Interest: The authors declare no conflict of interest.

References

1. Abakumov, G.A.; Nevodchikov, V.I. Thermo- and photomechanical effect on the crystals of free-radical complex. *Dokl. Akad. Nauk SSSR* **1982**, *266*, 1407–1410.
2. Jung, O.; Pierpont, C.G. Bistability and Low-Energy Electron Transfer in Cobalt Complexes Containing Catecholate and Semiquinone Ligands. *Inorg. Chem.* **1994**, *33*, 2227–2235. [CrossRef]
3. Abakumov, G.A.; Cherkasov, V.K.; Bubnov, M.P.; Ellert, O.G.; Dobrokhotova, Z.V.; Zakharov, L.N.; Struchkov, Y.T. Investigation of BpyCo(SQ)₂ by X-ray diffraction, magnetochemistry, and precision calorimetry. *Dokl. Akad. Nauk* **1993**, *328*, 332–335.
4. Broere, D.L.J.; Plessius, R.; van der Vlugt, J.I. New avenues for ligand-mediated processes—Expanding metal reactivity by the use of redox-active catechol, *o*-aminophenol and *o*-phenylenediamine ligands. *Chem. Soc. Rev.* **2015**, *44*, 6886–6915. [CrossRef] [PubMed]
5. Moussa, J.; Rager, M.N.; Chamoreau, L.M.; Ricard, L.; Amouri, H. Unprecedented π-Bonded Rhodio- and Iridio-*o*-Benzoquinones as Organometallic Linkers for the Design of Chiral Octahedral Bimetallic Assemblies. *Organometallics* **2009**, *28*, 397–404. [CrossRef]
6. Damas, A.; Gullo, M.P.; Rager, M.N.; Jutand, A.; Barbieri, A.; Amouri, H. Near-infrared room temperature emission from a novel class of Ru(II) heteroleptic complexes with quinonoid organometallic linker. *Chem. Commun.* **2013**, *49*, 3796–3798. [CrossRef] [PubMed]
7. Damas, A.; Ventura, B.; Axet, M.R.; Degli Esposti, A.; Chamoreau, L.-M.; Barbieri, A.; Amouri, H. Organometallic Quinonoid Linkers: A Versatile Tether for the Design of Panchromatic Ruthenium(II) Heteroleptic Complexes. *Inorg. Chem.* **2010**, *49*, 10762–10764. [CrossRef] [PubMed]
8. Damas, A.; Ventura, B.; Moussa, J.; Degli Esposti, A.; Chamoreau, L.-M.; Barbieri, A.; Amouri, H. Turning on Red and Near-Infrared Phosphorescence in Octahedral Complexes with Metalated Quinones. *Inorg. Chem.* **2012**, *51*, 1739–1750. [CrossRef] [PubMed]
9. Moussa, J.; Chamoreau, L.-M.; Degli Esposti, A.; Gullo, M.P.; Barbieri, A.; Amouri, H. Tuning Excited States of Bipyridyl Platinum(II) Chromophores with π-Bonded Catecholate Organometallic Ligands: Synthesis, Structures, TD-DFT Calculations, and Photophysical Properties. *Inorg. Chem.* **2014**, *53*, 6624–6633. [CrossRef] [PubMed]
10. Moussa, J.; Loch, A.; Chamoreau, L.-M.; Degli Esposti, A.; Bandini, E.; Barbieri, A.; Amouri, H. Luminescent Cyclometalated Platinum Complexes with π-Bonded Catecholate Organometallic Ligands. *Inorg. Chem.* **2017**, *56*, 2050–2059. [CrossRef] [PubMed]
11. Broere, D.L.J.; Plessius, R.; Tory, J.; Demeshko, S.; de Bruin, B.; Siegler, M.A.; Hartl, F.; van der Vlugt, J.I. Localized Mixed-Valence and Redox Activity within a Triazole-Bridged Dinucleating Ligand upon Coordination to Palladium. *Chem. Eur. J.* **2016**, *22*, 13965–13975. [CrossRef] [PubMed]
12. Sarkar, B.; Schweinfurth, D.; Deibel, N.; Weisser, F. Functional metal complexes based on bridging "imino"-quinonoid ligands. *Coord. Chem. Rev.* **2015**, *293–294*, 250–262. [CrossRef]

13. Pascal, S.; Siri, O. Benzoquinonediimine ligands: Synthesis, coordination chemistry and properties. *Coord. Chem. Rev.* **2017**, *350*, 178–195. [CrossRef]

14. Smith, G.F.; Cagle, F.W. The improved synthesis of 5-nitro-1,10-phenanthroline. *J. Org. Chem.* **1947**, *12*, 781–784. [CrossRef] [PubMed]

15. Masaki, Y.; Yoshihito, T.; Yasuyuki, Y.; Shigeyasu, K.; Ichiro, S. Synthesis and Properties of Diamino-Substituted Dipyrido [3,2-a: 2′,3′-c]phenazine. *Bull. Chem. Soc. Jpn.* **1992**, *65*, 1006–1011.

16. Ghosh, S.; Barve, A.C.; Kumbhar, A.A.; Kumbhar, A.S.; Puranik, V.G.; Datar, P.A.; Sonawane, U.B.; Joshi, R.R. Synthesis, characterization, X-ray structure and DNA photocleavage by *cis*-dichloro bis(diimine) Co(III) complexes. *J. Inorg. Biochem.* **2006**, *100*, 331–343. [CrossRef] [PubMed]

17. Boghaei, D.M.; Behzadian-Asl, F. Synthesis, characterization and fluorescence spectra of mononuclear Zn(II), Cd(II) and Hg(II) complexes with 1,10-phenanthroline-5,6-dione ligand. *J. Coord. Chem.* **2007**, *60*, 347–353. [CrossRef]

18. Conrad, R.C.; Rund, J.V. Effect of basicity of nonreacting ligands on the rate of reaction of dithiooxamide wth dichloro (phenanthroline) platinum(II) derivatives. *Inorg. Chem.* **1972**, *11*, 129–134. [CrossRef]

19. Girgis, A.Y.; Sohn, Y.S.; Balch, A.L. Preparation and oxidation of some quinone adducts of transition metal complexes. *Inorg. Chem.* **1975**, *14*, 2327–2331. [CrossRef]

20. Fox, G.A.; Bhattacharya, S.; Pierpont, C.G. Structural and electrochemical properties of binuclear complexes containing 1,10-phenanthroline-5,6-diolate as a bridging ligand. *Inorg. Chem.* **1991**, *30*, 2895–2899. [CrossRef]

21. Goss, C.A.; Abruna, H.D. Spectral, electrochemical and electrocatalytic properties of 1,10-phenanthroline-5,6-dione complexes of transition metals. *Inorg. Chem.* **1985**, *24*, 4263–4267. [CrossRef]

22. Murphy, D.M.; McNamara, K.; Richardson, P.; Sanchez-Romaguera, V.; Winpenny, R.E.P.; Yellowlees, L.J. Electrochemical and spectroelectrochemical studies of complexes of 1,10-phenanthroline-5,6-dione. *Inorg. Chim. Acta* **2011**, *374*, 435–441. [CrossRef]

23. Calderazzo, F.; Marchetti, F.; Pampaloni, G.; Passarelli, V. Co-ordination properties of 1,10-phenanthroline-5,6-dione towards group 4 and 5 metals in low and high oxidation states. *J. Chem. Soc. Dalton Trans.* **1999**, *24*, 4389–4396. [CrossRef]

24. Rei, O.; Tetsuaki, F.; Tohru, W.; Koji, T. Comparison of Basicity of the Diimine and Quinoid Group of 1,10-Phenanthroline-5,6-dione Ligated on Pt(II). *Bull. Chem. Soc. Jpn.* **2006**, *79*, 106–112.

25. Paw, W.; Eisenberg, R. Synthesis, Characterization, and Spectroscopy of Dipyridocatecholate Complexes of Platinum. *Inorg. Chem.* **1997**, *36*, 2287–2293. [CrossRef] [PubMed]

26. Calderazzo, F.; Pampaloni, G.; Passarelli, V. 1,10-Phenanthroline-5,6-dione as a building block for the synthesis of homo- and heterometallic complexes. *Inorg. Chim. Acta* **2002**, *330*, 136–142. [CrossRef]

27. Calucci, L.; Pampaloni, G.; Pinzino, C.; Prescimone, A. Transition metal derivatives of 1,10-phenanthroline-5,6-dione: Controlled growth of coordination polynuclear derivatives. *Inorg. Chim. Acta* **2006**, *359*, 3911–3920. [CrossRef]

28. Brechin, E.K.; Calucci, L.; Englert, U.; Margheriti, L.; Pampaloni, G.; Pinzino, C.; Prescimone, A. 1,10-Phenanthroline-5,6-dione complexes of middle transition elements: Mono- and dinuclear derivatives. *Inorg. Chim. Acta* **2008**, *361*, 2375–2384. [CrossRef]

29. Shavaleev, N.M.; Moorcraft, L.P.; Pope, S.J.A.; Bell, Z.R.; Faulkner, S.; Ward, M.D. Sensitized Near-Infrared Emission from Complexes of Yb[III], Nd[III] and Er[III] by Energy-Transfer from Covalently Attached Pt[II]-Based Antenna Units. *Chem. Eur. J.* **2003**, *9*, 5283–5291. [CrossRef] [PubMed]

30. Shavaleev, N.M.; Moorcraft, L.P.; Pope, S.J.A.; Bell, Z.R.; Faulkner, S.; Ward, M.D. Sensitised near-infrared emission from lanthanides using a covalently-attached Pt(II) fragment as an antenna group. *Chem. Commun.* **2003**, *10*, 1134–1135. [CrossRef]

31. Coucouvanis, D.; Jonasdottir, S.G.; Christodoulou, D.; Kim, C.G.; Kampf, J.W. Multifunctional macrocyclic ligands. Synthesis and characterization of nickel(II) and cobalt(II) macrocyclic-catechol complexes and their dimeric, antiferromagnetically coupled, semiquinone derivatives. *Inorg. Chem.* **1993**, *32*, 2987–2988. [CrossRef]

32. Jonasdottir, S.G.; Kim, C.G.; Coucouvanis, D. Macrocyclic catechol complexes as ligands in the synthesis of heterometallic supramolecules. *Inorg. Chem.* **1993**, *32*, 3591–3592. [CrossRef]

33. Jonasdottir, S.; Kim, C.-G.; Kampf, J.; Coucouvanis, D. Macrocyclic catecholate complexes as ligands. Synthesis, structural characterization and properties of the [MH$_2$ETC] and {[Ni(ETC)]Cu}$^{2-}$ complexes (M = Co, Ni; H$_4$ETC = the macrocyclic catechol, 2,3-ethylene-5,6:13,14-di-(5′-methylbzo)-9, 10-(4′,5′-diolbzo)-[14]-1,4,8,11-[N$_4$]-7,12-diene). *Inorg. Chim. Acta* **1996**, *243*, 255–270.

34. Malinak, S.M.; Coucouvanis, D. Synthesis and Characterization of [Mo$_2$O$_5$]$^{2+}$-Bridged Complexes Containing Cofacially-Oriented, Catechol-Functionalized Macrocyclic and SALPHEN Ligands. *Inorg. Chem.* **1996**, *35*, 4810–4811. [CrossRef] [PubMed]

35. Malinak, S.M.; Rosa, D.T.; Coucouvanis, D. A New Class of Complexes Possessing Cofacially-Oriented, Planar, Metal-Containing Subunits. Synthesis, Characterization, and Reactivity of [(MoO$_2$)$_2$(μ-O)]$^{2+}$-Linked, Catechol-Functionalized, Tetraazamacrocyclic and Salicylideneamine Complexes. *Inorg. Chem.* **1998**, *37*, 1175–1190. [CrossRef] [PubMed]

36. Schley, M.; Lönnecke, P.; Hey-Hawkins, E. Monometallic and heterobimetallic complexes derived from salen-type ligands. *J. Organomet. Chem.* **2009**, *694*, 2480–2487. [CrossRef]

37. Weber, B.; Obel, J. Synthesis and Characterisation of a New Schiff-Base-like Ligand and its Iron(II) Complexes. *Zeitschrift für Anorganische und Allgemeine Chemie* **2009**, *635*, 2474–2479. [CrossRef]

38. Weber, B.; Obel, J.; Henner-Vásquez, D.; Bauer, W. Two New Iron(II) Spin-Crossover Complexes with N$_4$O$_2$ Coordination Sphere and Spin Transition around Room Temperature. *Eur. J. Inorg. Chem.* **2009**, *2009*, 5527–5534. [CrossRef]

39. Bauer, W.; Lochenie, C.; Weber, B. Synthesis and characterization of 1D iron(II) spin crossover coordination polymers with hysteresis. *Dalton Trans.* **2014**, *43*, 1990–1999. [CrossRef] [PubMed]

40. Weber, B.; Obel, J.; Lorenz, L.R.; Bauer, W.; Carrella, L.; Rentschler, E. Control of Exchange Interactions in Trinuclear Complexes Based on Orthogonal Magnetic Orbitals. *Eur. J. Inorg. Chem.* **2009**, *2009*, 5535–5540. [CrossRef]

41. Coucouvanis, D.; Paital, A.R.; Zhang, Q.; Lehnert, N.; Ahlrichs, R.; Fink, K.; Fenske, D.; Powell, A.K.; Lan, Y. Synthesis, electronic structure, and structural characterization of the new, "non-innocent" 4,5-dithio-catecholate ligand, its metal complexes, and their oxidized 4,5-dithio-*o*-quinone derivatives. *Inorg. Chem.* **2009**, *48*, 8830–8844. [CrossRef] [PubMed]

42. Cherkasov, V.K.; Abakumov, G.A.; Fukin, G.K.; Klementyeva, S.V.; Kuropatov, V.A. Sterically Hindered *o*-Quinone Annulated with Dithiete: A Molecule Comprising Diolate and Dithiolate Coordination Sites. *Chem. Eur. J.* **2012**, *18*, 13821–13827. [CrossRef] [PubMed]

43. Martyanov, K.A.; Cherkasov, V.K.; Abakumov, G.A.; Samsonov, M.A.; Khrizanforova, V.V.; Budnikova, Y.H.; Kuropatov, V.A. New sterically-hindered *o*-quinones annelated with metal-dithiolates: Regiospecificity in oxidative addition reactions of a bifacial ligand to the Pd and Pt complexes. *Dalton Trans.* **2016**, *45*, 7400–7405. [CrossRef] [PubMed]

44. Martyanov, K.A.; Cherkasov, V.K.; Abakumov, G.A.; Baranov, E.V.; Shavyrin, A.S.; Kuropatov, V.A. Regioisomerism in coordination chemistry: Oxidative addition of a bifunctional ligand to palladium, stabilized with 1,2-bis (diphenylphosphino)ethane. *Dalton Trans.* **2017**, *46*, 16783–16786. [CrossRef] [PubMed]

45. Razuvaev, G.A.; Abakumov, G.A.; Teplova, I.A.; Shalnova, K.G.; Cherkasov, V.K. Palladium and platinum paramagnetic complexes formed by oxidation of catecholate derivatives of these elements. *Inorg. Chim. Acta* **1981**, *53*, L267-L269. [CrossRef]

46. Perepichka, D.F.; Bryce, M.R.; Batsanov, A.S.; McInnes, E.J.L.; Zhao, J.P.; Farley, R.D. Engineering a remarkably low HOMO–LUMO gap by covalent linkage of a strong π-donor and a π-acceptor-tetrathiafulvalene-σ-polynitrofluorene diads: Their amphoteric redox behavior, electron transfer and spectroscopic properties. *Chem. Eur. J.* **2002**, *8*, 4656–4669. [CrossRef]

47. Kuropatov, V.; Klementieva, S.; Fukin, G.; Mitin, A.; Ketkov, S.; Budnikova, Y.; Cherkasov, V.; Abakumov, G. Novel method for the synthesis of functionalized tetrathiafulvalenes, an acceptor–donor–acceptor molecule comprising of two o-quinone moieties linked by a TTF bridge. *Tetrahedron* **2010**, *66*, 7605–7611. [CrossRef]

48. Kuropatov, V.A.; Klementieva, S.V.; Poddel'sky, A.I.; Cherkasov, V.K.; Abakumov, G.A. ESR study of paramagnetic derivatives of sterically hindered di-*o*-quinone with the tetrathiafulvalene bridge. *Russ. Chem. Bull.* **2010**, *59*, 1698–1706. [CrossRef]

49. Klementieva, S.V.; Kuropatov, V.A.; Fukin, G.K.; Romanenko, G.V.; Bogomyakov, A.S.; Cherkasov, V.K.; Abakumov, G.A. Mono- and Binuclear Dimethylthallium(III) Complexes with *o*-Benzoquinone-TTF-*o*-Benzoquinone Ligand; Synthesis, Spectroscopy and X-ray Study. *Zeitschrift für Anorganische und Allgemeine Chemie* **2011**, *637*, 232–241. [CrossRef]

50. Pointillart, F.; Klementieva, S.; Kuropatov, V.; Le Gal, Y.; Golhen, S.; Cador, O.; Cherkasov, V.; Ouahab, L. A single molecule magnet behaviour in a D_{3h} symmetry Dy(III) complex involving a quinone-tetrathiafulvalene-quinone bridge. *Chem. Commun.* **2012**, *48*, 714–716. [CrossRef] [PubMed]

51. Pointillart, F.; Kuropatov, V.; Mitin, A.; Maury, O.; Le Gal, Y.; Golhen, S.; Cador, O.; Cherkasov, V.; Ouahab, L. Lanthanide-Based Dinuclear Complexes Involving an *o*-Quinone–Tetrathiafulvalene–*o*-Quinone Bridging Ligand: X-ray Structures, Magnetic and Photophysical Properties. *Eur. J. Inorg. Chem.* **2012**, *2012*, 4708–4718. [CrossRef]

52. Yamashita, Y.; Kobayashi, Y.; Miyashi, T. *p*-Quinodimethane Analogues of Tetrathiafulvalene. *Angew. Chem. Int. Ed. Engl.* **1989**, *28*, 1052–1053. [CrossRef]

53. Chalkov, N.O.; Cherkasov, V.K.; Abakumov, G.A.; Romanenko, G.V.; Ketkov, S.Y.; Smolyaninov, I.V.; Starikov, A.G.; Kuropatov, V.A. Compactly Fused *o*-Quinone-Extended Tetrathiafulvalene-*o*-Quinone Triad—A Redox-Amphoteric Ligand. *Eur. J. Org. Chem.* **2014**, *2014*, 4571–4576. [CrossRef]

54. Chalkov, N.O.; Cherkasov, V.K.; Abakumov, G.A.; Starikov, A.G.; Kuropatov, V.A. EPR spectroscopy study of di-*o*-quinone bridged by π-extended TTF: Redox behavior and binding modes as a ligand. *New J. Chem.* **2016**, *40*, 1244–1249. [CrossRef]

55. Chalkov, N.O.; Cherkasov, V.K.; Abakumov, G.A.; Starikov, A.G.; Kuropatov, V.A. Protonated paramagnetic redox forms of di-*o*-quinone bridged with *p*-phenylene-extended TTF: A EPR spectroscopy study. *Beilstein J. Org. Chem.* **2016**, *12*, 2450–2456. [CrossRef] [PubMed]

56. Robin, M.B.; Day, P. Mixed Valence Chemistry-A Survey and Classification. *Adv. Inorg. Chem. Radiochem.* **1967**, *10*, 247–422.